

Abstract

There is scientific and industrial interest in understanding how geologic faults respond to transient sources of fluid. Natural and artificial sources of fluid that elevate pore fluid pressure on the fault frictional interface, which may induce slip. Here we consider a simple boundary value problem to provide an elementary model of the physical process and to provide a benchmark for numerical solution procedures. We examine the slip of a fault that is an interface of two elastic half-spaces. Injection is modeled as a line source at constant pressure and fluid pressure is assumed to diffuse along the interface. The resulting problem is an integro-differential equation governing fault slip, which has a single dimensionless parameter. The expansion of slip is self-similar and the rupture front propagates at a factor λ of the diffusive lengthscale \sqrt{at} . We identify two asymptotic regimes corresponding to λ being small or large and perform a perturbation expansion in each limit. For large λ , in the regime of a so-called critically stressed fault, a boundary layer emerges on the diffusive lengthscale, which lags far behind the rupture front. We demonstrate higher-order matched asymptotics for the integro-differential equation, and in doing so, we derive a multipole expansion method to capture successive orders of influence on the outer problem for fault slip for a driving force that is small relative to the crack dimensions. Asymptotic expansions are compared to accurate numerical solutions to the full problem, which are tabulated to high precision.

1. Introduction

A source of fluid in the subsurface can drive the rupture of a geologic fault by locally reducing the fault's frictional shear strength below an ambient level of shear stress such that fault must slide. The fluid source may be natural, such as from mineral dehydration of subducted sediments or from a mantle source, or artificial, such as from the subsurface injection of fluids at kilometer scale depths for the disposal of wastewater or for the enhancement of permeability in geothermal systems. Despite wide interest, simple solutions for fluid-induced fault slip are scarce.

Here we present an elementary model for fault response to fluid injection. We consider a planar fault in an unbounded, linear-elastic medium under a uniform state of stress prior to injection. Quasi-static deformation is restricted to in-plane or anti-plane, such that the corresponding fault slip is mode II or mode III rupture. We use a boundary integral formulation to relate the crack-face displacement and traction. Injection is modeled as a line source of fluids at constant pressure following which fluid migration, and the concomitant rise in pore fluid pressure, is restricted to occur along the fault plane. The fault strength is frictional and is the product of a constant coefficient of friction and the local effective normal stress, the difference between the fault-normal traction and the local pore fluid pressure.

This problem was presented in *Bhattacharya and Viesca* [2019] and is a variation of one considered in depth by *Garagash and Germanovich* [2012] (hereafter referred to as GG12). GG12 examined the response to injection of a fault under the same elastic and fluid conditions considered here. However, GG12 considered a fault friction coefficient that weakens with slip, a feature that gives rise to rich behavior, including the possibility of dynamic rupture nucleation and arrest, corresponding to an earthquake source. GG12 found two end-member regimes corresponding to marginally pressurized and critically stressed faults, which reflect the pre-injection state of stress. The authors showed that these regimes lead to a rupture front lagging or outpacing fluid diffusion, respectively, and that, in the critically stressed regime, fault slip can be described by a boundary-layer analysis. However the slip-dependent strength in that problem required numerical solution, even in end-member regimes, and growth of the slipping region was non-trivial and dependent on at least two problem parameters.

Adopting constant Coulomb friction leads to stable growth of fault rupture. Foremost, the propagation of fault slip occurs in self-similar manner in response to a self-similar source. Additionally,

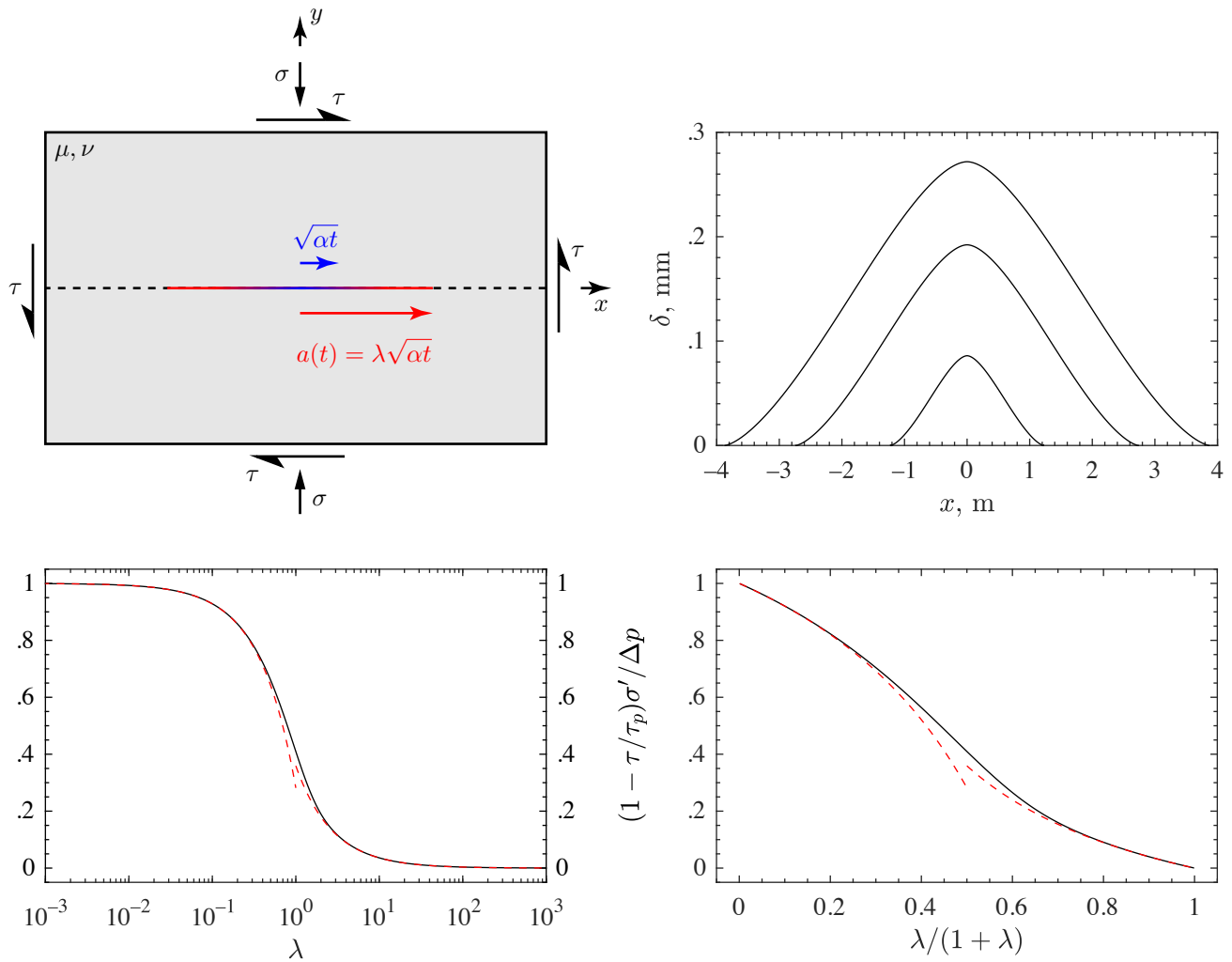


Fig. 1. Counter-clockwise: (top left) Unbounded elastic body containing a fault, loaded remotely with fault-normal and shear stress σ , τ . Fluid injection at $x = 0$ diffuses along fault as $\sqrt{\alpha t}$, inducing quasi-static slip out to a distance $a(t)$. Fault has constant friction coefficient f . (bottom left) Black: relation between rupture growth factor λ and a parameter reflecting the initial state of stress and injection pressure, where $\sigma' = \sigma - p_o$ and p_o is pre-injection fault fluid pressure. Dashed: asymptotic behaviors, eqs. (5) and (8). (bottom right) Same as bottom left, with abscissa arranged to occupy a finite interval. (top right) Plot of self-similar slip distributions at three instants in time after the start of injection, $t = 1$, 5 , and 10 min., for the specific choices $\sigma = 50$ MPa, $\tau = 12$ MPa, $p_o = 20$ MPa, $\Delta p = 12$ MPa, $f = 0.5$, $\alpha_{hy} = 0.01$ m²/s, $\mu = 30$ GPa, $\nu = 1/4$, $\mu' = 20$ GPa. For these choices, the parameter $(1 - \tau/\tau_p)\sigma'/\Delta p = 0.5$. The corresponding self-similar slip distribution and factor λ are given in Table 1.

the problem has a single dimensionless parameter, with the same two end-member regimes as in the problem considered by GG12. The simpler problem admits closed-form perturbation expansion in these regimes, and readily allows for higher-order asymptotic matching of the boundary-layer problem in the critically stressed regime. In this regime, where the rupture front races ahead of the elevated fluid pressure distribution, the problem provides for the development of a multipole expansion technique to consider the higher-order source effects. The problem is also amenable to accurate numerical solutions for the cases intervening the two end-member regimes and we provide tabulated solutions to high precision.

We begin by providing a problem statement and summary of asymptotic solutions to leading order in the critically stressed and marginally pressurized limits. Subsequently, we return to the full problem and summarize its solution. Finally, we revisit the end-member regimes and derive the asymptotic solutions to second order. In the marginally pressurized limit, the solution is a single perturbation expansion. In the critically stressed limit, inner and outer perturbation expansions are found and the two solutions are matched to construct a composite solution. We compare the asymptotic expansions to numerical solutions to the full problem throughout.

2. Problem formulation and solution summary

We consider a fault plane lying on $y = 0$ and a line fluid source of constant pressure located at $x = 0$, along the z axis. The medium containing the fault is linearly elastic and the deformation may be in-plane or anti-plane. The in-plane case is illustrated in Fig. 1 (top left). The shear modulus of the medium is μ and the Poisson ratio ν . We define the effective elastic modulus $\mu' = \mu/[2(1 - \nu)]$ for in-plane (mode-II) case and $\mu' = \mu/2$ for anti-plane (mode-III) case. We denote the initial (pre-injection) fault shear stress τ (in-plane or anti-plane), the fault friction coefficient f , the initial pore fluid pressure on interface p_o , the initial total fault-normal compressive stress σ , and the initial effective normal stress $\sigma' = \sigma - p_o$. The initial fault strength is $\tau_p = f\sigma'$.

We consider one-dimensional diffusion of pore fluid pressure along the fault

$$p_t = \alpha_{hy} p_{xx}$$

where α_{hy} is the hydraulic diffusivity of the fault core and where the pore pressure is subject to the conditions of the initial state and injection at constant pressure Δp at $x = 0$,

$$p(x, 0) = p_o, \quad p(0, t > 0) = \Delta p$$

the known solution to which is

$$p(x, t) = p_o + \Delta p \operatorname{erfc}(|x|/\sqrt{\alpha t}) \quad (1)$$

where we adopt a nominal diffusivity

$$\alpha = 4\alpha_{hy}$$

The fault obeys a Coulomb friction law: the local shear strength of the fault τ_s is a constant proportion of the local effective normal stress, with a constant coefficient of friction f

$$\tau_s(x, t) = f[\sigma - p(x, t)] \quad (2)$$

Where sliding occurs, this strength must equal the shear stress on the fault. The shear stress can be decomposed into a sum of the initial shear stress τ plus quasi-static changes due to a distribution of slip δ , such that the stress-strength condition is

$$\tau_s(x, t) = \tau + \frac{\mu'}{\pi} \int_{-a(t)}^{a(t)} \frac{\partial \delta(s, t)/\partial s}{s - x} ds \quad (3)$$

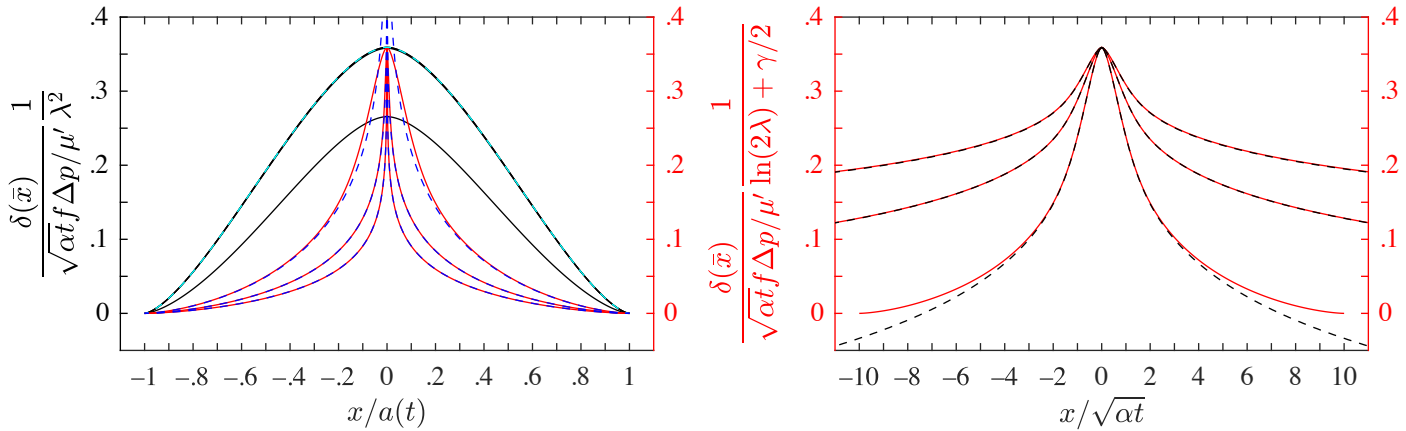


Fig. 2. (left) Self-similar distributions of slip δ with distance from injection point x , which is scaled by the crack length $a(t) = \lambda\sqrt{\alpha t}$. Each distribution corresponds to one value of λ in the range $\lambda = 10^{-3}, 10^{-2}, \dots, 10^3$. To facilitate comparisons, slip is scaled differently for black and red curves. Black curves correspond to $\lambda = 10^{-3}, 10^{-2}, 10^{-1}, 10^0$ from top to bottom, with the first three indistinguishable on this scale; red curves correspond to $\lambda = 10^1, 10^2, 10^3$ from top to bottom. Cyan-dashed: solution for small λ , eq. (6). Blue-dashed: “outer” solutions for large λ , eq. (9). **(right)** For large values of λ , the distribution of slip is plotted over distances scaled by $\sqrt{\alpha t}$, which is much smaller than the crack length $a(t)$. This “inner” behavior is described by eq. (10), a single numerical solution shown here as black-dashed curves. Curves correspond to $\lambda = 10^1, 10^2, 10^3$ from bottom to top.

where $x = \pm a(t)$ are the crack-tip locations.

After non-dimensionalizing, the problem is found to have a sole parameter

$$\left(1 - \frac{\tau}{\tau_p}\right) \frac{\sigma'}{\Delta p} \quad (4)$$

that is bound between 0 and 1. The upper bound denotes a marginally pressurized fault, where the fluid pressure increase is just sufficient to initiate sliding: $f[\sigma - (p_o + \Delta p)] = \tau$. The lower bound denotes a critically stress fault, where the initial shear stress is equal to the initial shear strength: $\tau = \tau_p$.

The solution consists of a self-similar distribution of slip, in which the crack front grows as

$$a(t) = \lambda\sqrt{\alpha t}$$

and the slip distribution can be written as

$$\delta(x, t) \Rightarrow \delta(\bar{x})$$

where the similarity coordinate is

$$\bar{x} = x/a(t)$$

The factor λ , to be solved for, determines whether the crack lags ($\lambda < 1$) or outpaces ($\lambda > 1$) the diffusion of pore pressure, which stretches as $\sqrt{\alpha t}$. λ depends uniquely on the sole parameter (4), and that dependence is illustrated in Fig. 1b and tabulated at the top of Table 1. The self-similar profile of slip, as it depends on $|x|/a(t)$, is also presented in the bottom of Table 1 for several values of the parameter (4). Scaled plots of the self-similar profile for various values of λ are shown in Fig.

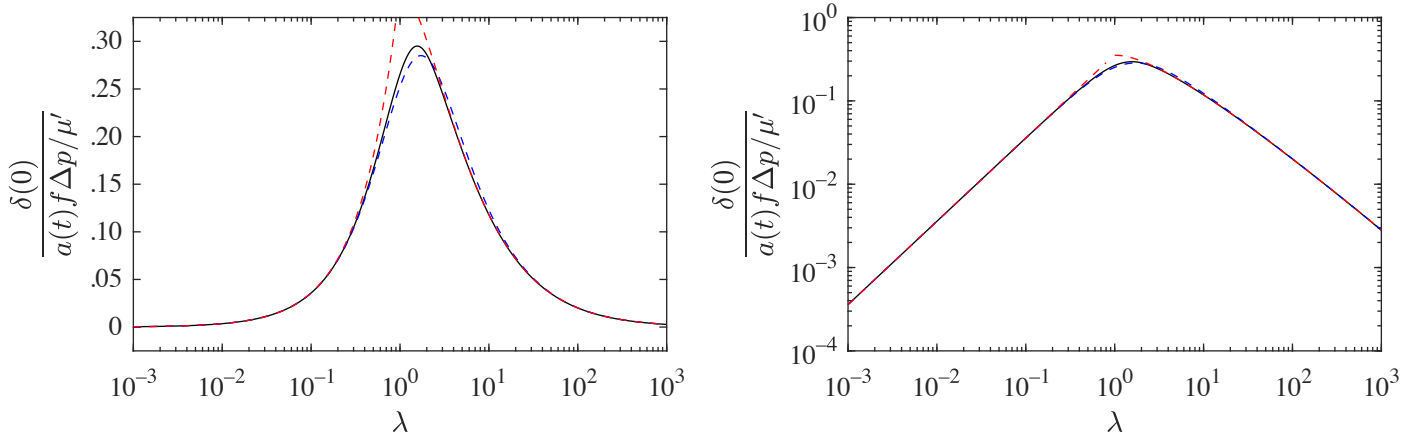


Fig. 3. The maximum slip, which occurs at $x = 0$, as it relates to the factor λ shown as (**top**) linear (**left**) semi-log and (**right**) log-log plots. Red-dashed: end-member scalings at small λ , eq. (7), and at large λ , eq. (12). Blue-dashed: approximation of $\delta(0)$ for all λ , eq. (14).

2. In the limit that the parameter (4) approaches its end-member values, closed-form expressions for λ and δ are available and provided below.

2.1 Marginally pressurized faults: $\tau \rightarrow f(\sigma' - \Delta p)$

In this limit, the parameter $(1 - \tau/\tau_p) \sigma'/\Delta p \rightarrow 1$, the factor $\lambda \ll 1$ (i.e., the rupture lags the diffusion of pore fluid pressure), and the relation between the two follows the asymptotic expansion

$$(1 - \tau/\tau_p) \sigma'/\Delta p \approx 1 - \frac{4}{\pi^{3/2}} \lambda - O(\lambda^3) \quad (5)$$

The slip distribution in this limit is

$$\delta(\bar{x}) \approx \frac{\lambda^2 \sqrt{\alpha t} f \Delta p}{\mu'} \frac{2}{\pi^{3/2}} \left(\sqrt{1 - \bar{x}^2} - \bar{x}^2 \operatorname{atanh} \sqrt{1 - \bar{x}^2} \right) + O(\lambda^4) \quad (6)$$

and the accumulation of slip at the center is

$$\delta(0) \approx \frac{2}{\pi^{3/2}} \frac{\lambda^2 \sqrt{\alpha t} f \Delta p}{\mu'} + O(\lambda^4) \quad (7)$$

2.2 Critically stressed faults: $\tau \rightarrow \tau_p$

In this limit $(1 - \tau/\tau_p) \sigma'/\Delta p \rightarrow 0$, $\lambda \gg 1$ (i.e., the rupture outpaces the diffusion of fluid pressure), and the asymptotic relation is

$$(1 - \tau/\tau_p) \sigma'/\Delta p \approx \frac{2}{\pi^{3/2}} \frac{1}{\lambda} + O(\lambda^{-3}) \quad (8)$$

Similarly to the problem considered by *Garagash and Germanovich* [2012], the solution for slip can be decomposed into an outer solution on distances comparable to the rupture distance $a(t)$, and an inner solution on distances comparable to the diffusion lengthscale $\sqrt{\alpha t}$. The two solutions are matched at an intermediate distance.

The outer solution for the slip distribution is

$$\delta(\bar{x}) \approx \frac{\sqrt{\alpha t} f \Delta p}{\mu'} \frac{2}{\pi^{3/2}} \left(\operatorname{atanh} \sqrt{1 - \bar{x}^2} - \sqrt{1 - \bar{x}^2} \right) + O(\lambda^{-2}) \quad (9)$$

where \bar{x} is the similarity coordinate used above.

The inner solution is given by the expression

$$\delta(x/\sqrt{\alpha t}) \approx \delta(0) - \underline{\frac{\sqrt{\alpha t} f \Delta p}{\mu'} \int_0^{x/\sqrt{\alpha t}} \left[\frac{1}{\pi} \int_{-\infty}^{\hat{s}} \frac{\operatorname{erfc}(|\hat{s}|)}{\hat{x} - \hat{s}} d\hat{s} \right] d\hat{x}} + O(\lambda^{-2}) \quad (10)$$

The underlined portion is evaluated numerically and provided as a supplementary function $f(x/\sqrt{\alpha t})$ in Table 2 with the similarity coordinate

$$\hat{x} = \frac{x}{\sqrt{\alpha t}}$$

For large distances $x/\sqrt{\alpha t}$, f behaves as

$$f(\hat{x}) \approx \frac{2}{\pi^{3/2}} \left(\ln |\hat{x}| + \frac{\gamma}{2} + 1 \right) + O(\hat{x}^{-2}) \quad (11)$$

where $\gamma = 0.57721566\dots$ is the Euler-Maraschoni constant. Using this asymptotic behavior to match the inner solution at large $x/\sqrt{\alpha t}$ with the outer solution at small $x/a(t)$ provides the slip at the center

$$\delta(0) \approx \frac{\sqrt{\alpha t} f \Delta p}{\mu'} \frac{2}{\pi^{3/2}} [\ln(2\lambda) + \gamma/2 + O(\lambda^{-2})] \quad (12)$$

in the large λ limit.

Other properties of $f(x/\sqrt{\alpha t})$ include

$$f''(\hat{x}) = -\frac{2}{\pi^{3/2}} \exp(-\hat{x}^2) \operatorname{Ei}(\hat{x}^2)$$

where $\operatorname{Ei}(x) = -\int_{-x}^{\infty} \exp(-u)/u du$ is the exponential integral, and in the limit that $x/\sqrt{\alpha t}$ is small, f behaves as

$$f(\hat{x}) \approx \frac{2}{\pi^{3/2}} \hat{x}^2 \left(\ln \frac{1}{|\hat{x}|} - \frac{\gamma}{2} + \frac{3}{2} \right) + O(\hat{x}^4 \ln |\hat{x}|) \quad (13)$$

2.3 Accumulation of slip at the injection point

Figs. 3 and 4 show the solution for the peak slip, located at the injection point, as it depends on the parameter (4) or the factor λ . An approximation of peak slip at the injection point that respects the asymptotic behavior at both critically stressed and marginally pressurized limits—eqs. (7) and (12)—and is to within 5% error over the intervening range of λ , is

$$\delta(0) \approx \frac{\lambda \sqrt{\alpha t} f \Delta p}{\mu'} \frac{2}{\pi^{3/2}} \frac{\lambda}{1 + \lambda^2 / [\ln(6 + 2\lambda) + \gamma/2]} \quad (14)$$

Table 1. Tabulation of the dependence of both factor λ and self-similar slip distribution $\delta(\bar{x})$ on the problem parameter $(1 - \tau/\tau_p) \sigma'/\Delta p$. Note abbreviation: $T = (1 - \tau/\tau_p) \sigma'/\Delta p$.

$(1 - \tau/\tau_p) \sigma'/\Delta p$	$\rightarrow 0$	0.1	0.2	0.3	0.4	0.5	0.6	0.7	0.8	0.9	$\rightarrow 1$
λ	$(2/\pi^{3/2})/T$	3.6405156	1.9125140	1.3474240	1.0252441	0.79160693	0.60122936	0.43513219	0.28337740	0.13981270	$(\pi^{3/2}/4)(1 - T)$
$ x /a(t)$	$\delta/(\sqrt{\alpha t} f \Delta p / \mu')$	$\delta/(\lambda \sqrt{\alpha t} f \Delta p / \mu')$									
0	$(2/\pi^{3/2})[\ln(2\lambda) + \gamma/2]$	0.22235814	0.28884483	0.29158012	0.26854750	0.23366202	0.19225196	0.14690288	0.099114755	0.049891607	0.35917424
.05	0.96600080	0.21293697	0.28287092	0.28705167	0.26495909	0.23081724	0.19005163	0.14529019	0.098055692	0.049366583	0.35541318
.10	0.71771469	0.19406542	0.26977998	0.27684966	0.25676095	0.22426165	0.18495186	0.14153779	0.095585199	0.048140087	0.34662298
.15	0.57320909	0.17141546	0.25241461	0.26293875	0.24543311	0.21513089	0.17781153	0.13626551	0.092106171	0.046410685	0.33422335
.20	0.47146496	0.14804366	0.23237418	0.24641194	0.23179150	0.20404685	0.16909871	0.12980996	0.087836899	0.044285816	0.31898215
.25	0.39336448	0.12579403	0.21080933	0.22806232	0.21642674	0.19145812	0.15914994	0.12241251	0.082933625	0.041842292	0.30144813
.30	0.33039758	0.10566200	0.18860371	0.20851874	0.19981014	0.17772295	0.14823375	0.11426559	0.077520767	0.039141242	0.28205787
.35	0.27803088	0.088034290	0.16644630	0.18830074	0.18233746	0.16314401	0.13657762	0.10553231	0.071703840	0.036234507	0.26118168
.40	0.23356530	0.07289864	0.14486896	0.16784610	0.16435133	0.14798653	0.12438207	0.096356965	0.065576337	0.033168065	0.23914800
.45	0.19526763	0.060023208	0.12427123	0.14752660	0.14615421	0.13248893	0.11182922	0.086871368	0.059223968	0.029984140	0.21625871
.50	0.16196334	0.049088021	0.10494029	0.12765847	0.12801685	0.11686999	0.099088536	0.077199247	0.052727610	0.026722691	0.19279968
.55	0.13282499	0.039772618	0.087069279	0.10851017	0.11018427	0.101334019	0.086321205	0.067459621	0.046165603	0.023422573	0.16904926
.60	0.10725384	0.031798805	0.070774899	0.090309083	0.092880849	0.086075209	0.073683848	0.057769761	0.039615810	0.020122586	0.14528583
.65	0.084810067	0.024945699	0.056114600	0.073248018	0.076314980	0.071281873	0.061332237	0.048248183	0.033157715	0.016862563	0.12179568
.70	0.065170463	0.019048185	0.043103256	0.057492242	0.060684332	0.057141201	0.049425558	0.039018155	0.026874910	0.013684652	0.098882348
.75	0.048103357	0.013988831	0.043103256	0.043187811	0.046182579	0.043845559	0.038132126	0.030212417	0.020858460	0.010635068	0.076879363
.80	0.033456068	0.0096894840	0.021971389	0.030472711	0.033009402	0.031602114	0.027638158	0.021980444	0.015212073	0.0077667764	0.056169753
.85	0.021154984	0.0061062150	0.013816179	0.019494061	0.021387701	0.020649782	0.018163273	0.014501247	0.010061206	0.0051442208	0.037220404
.90	0.011226140	0.0032311841	0.0072858109	0.010440840	0.011599155	0.011294788	0.0099929633	0.0080100955	0.0055720081	0.0028531253	0.020653307
.95	0.0038742471	0.0011124332	0.0024976528	0.0036291987	0.0040812723	0.0040083095	0.0035674726	0.0028713219	0.0020027229	0.0010270500	0.0074383239
1	0	0	0	0	0	0	0	0	0	0	0

Table 2. Tabulation of $f(x/\sqrt{\alpha t})$. Note discretization: $|x|/\sqrt{\alpha t} = \tan(\pi n/128)$.

n	$ x /\sqrt{\alpha t}$	$f(x/\sqrt{\alpha t})$	n	$ x /\sqrt{\alpha t}$	$f(x/\sqrt{\alpha t})$	n	$ x /\sqrt{\alpha t}$	$f(x/\sqrt{\alpha t})$	n	$ x /\sqrt{\alpha t}$	$f(x/\sqrt{\alpha t})$
0	0	0	16	0.41421356	0.12611233	32	1	0.39580461	48	2.4142136	0.76759781
1	0.024548622	0.0010645142	17	0.44326951	0.13933575	33	1.0503328	0.41648953	49	2.5924025	0.7949501
2	0.049126850	0.0036608823	18	0.47296478	0.15306718	34	1.1033300	0.43755981	50	2.7948128	0.82355843
3	0.073764432	0.0074561611	19	0.50335770	0.16730037	35	1.1592779	0.45899714	51	3.0270432	0.85359380
4	0.098491403	0.012278829	20	0.53451114	0.18203004	36	1.2185035	0.48078204	52	3.2965582	0.88542014
5	0.12333824	0.018013946	21	0.56649300	0.19725163	37	1.2813816	0.50289466	53	3.6135357	0.91943717
6	0.14833599	0.024577096	22	0.59937693	0.21296104	38	1.3483439	0.52531586	54	3.9922238	0.95614458
7	0.17351646	0.031903213	23	0.63324302	0.22915436	39	1.4198909	0.54802878	55	4.4532022	0.99618834
8	0.19891237	0.039940676	24	0.66817864	0.24582765	40	1.4966058	0.57102094	56	5.0273395	1.0404337
9	0.22455751	0.048647765	25	0.70427946	0.26297665	41	1.5791726	0.59428697	57	5.7631420	1.0900859
10	0.25048696	0.057990359	26	0.74165054	0.28059656	42	1.6683992	0.61783187	58	6.7414524	1.1469030
11	0.27673727	0.067940342	27	0.78040766	0.29868178	43	1.7652469	0.64167499	59	8.1077858	1.2136044
12	0.30334668	0.078474446	28	0.82067879	0.31722565	44	1.8708684	0.66585435	60	10.153170	1.2947397
13	0.33035538	0.089573374	29	0.86260593	0.33622021	45	1.9866588	0.69043124	61	13.556669	1.3988316
14	0.35780572	0.10122112	30	0.90634717	0.35565599	46	2.1143224	0.71549463	62	20.355468	1.5450076
15	0.38574257	0.11340443	31	0.95207915	0.37552179	47	2.2559639	0.74116509	63	40.735483	1.7942933

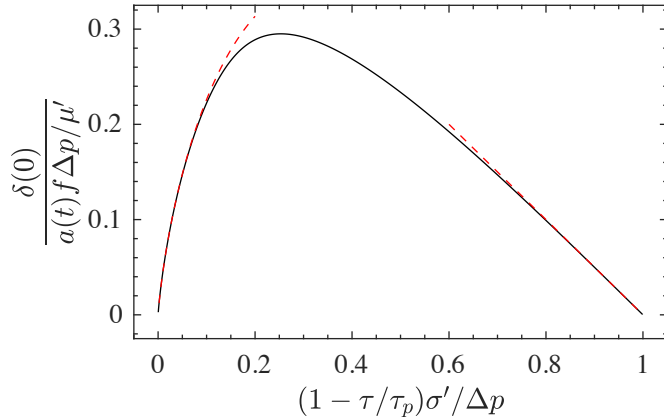


Fig. 4. The peak slip as it relates to the problem parameter $(1 - \tau/\tau_p)\sigma'/\Delta p$. Red-dashed: scalings as the parameter approaches its bounds, derived from eqs. (7) and (12) and the asymptotic relations between the parameter and λ , eqs. (5) and (8).

3. Non-dimensionalization and solution to full problem

Combining eqs. (1)–(3) and rearranging leads to the non-dimensionalized equation

$$\left(1 - \frac{\tau}{\tau_p}\right) \frac{\sigma'}{\Delta p} - \operatorname{erfc}|\lambda\bar{x}| = -\frac{1}{\pi} \int_{-1}^1 \frac{d\bar{\delta}/d\bar{s}}{\bar{x} - \bar{s}} d\bar{s} \quad (15)$$

where we have used $x = a(t)\bar{x}$, $a(t) = \lambda\sqrt{at}$, and $\delta(x, t) = \bar{\delta}[x/a(t)]a(t)f\Delta p/\mu'$. The solution we seek is the slip distribution $\bar{\delta}$ and the crack-growth prefactor λ , including their dependence on the problem parameter $(1 - \tau/\tau_p)/\sigma'/\Delta p$.

We begin by looking for the solution for λ . To do so, we first note that to avoid a singularity in shear stress ahead of the crack tips, which is necessary because the Coulomb friction requirement implies a finite shear strength of the interface, the crack-tip stress intensity factors of the rupture must be zero. This condition implies (Appendix A)

$$\left(1 - \frac{\tau}{\tau_p}\right) \frac{\sigma'}{\Delta p} = \frac{1}{\pi} \int_{-1}^1 \frac{\operatorname{erfc}|\lambda x|}{\sqrt{1-x^2}} dx \quad (16)$$

which provides a direct relation between the problem parameter and λ . This relation is easily determined numerically since, for a given λ , the integrand on the right hand side can be evaluated by Gauss-Chebyshev quadrature. The behavior at large and small values of λ , eqs. 5 and 8, is found by asymptotic approximation of the integral.

To solve for $\bar{\delta}$, we note that (15) may be inverted for $d\bar{\delta}/d\bar{x}$ (Appendix A)

$$\frac{d\bar{\delta}}{d\bar{x}} = -\frac{\sqrt{1-\bar{x}^2}}{\pi} \int_{-1}^1 \frac{\operatorname{erfc}|\lambda\bar{s}|}{\sqrt{1-\bar{s}^2}} \frac{1}{\bar{x}-\bar{s}} d\bar{s} \quad (17)$$

For a given λ the right hand side may be numerically evaluated and integrated to arrive to $\bar{\delta}(\bar{x})$ using a Gauss-Chebyshev quadrature for singular integrals [Erdogan et al., 1973; Viesca and Garagash, 2012].

4. Solution in the marginally pressurized limit

For $\lambda \ll 1$, we may use the expansion of the function

$$\operatorname{erfc}|\lambda\bar{x}| \approx 1 - \frac{2}{\sqrt{\pi}}|\lambda\bar{x}| + \frac{2}{3\sqrt{\pi}}|\lambda\bar{x}|^3 + \dots \quad (18)$$

to expand the integral in eq. (16) as

$$\left(1 - \frac{\tau}{\tau_p}\right) \frac{\sigma'}{\Delta p} = \int_{-1}^1 \frac{\operatorname{erfc}|\lambda x|}{\sqrt{1-x^2}} dx \approx 1 - \frac{4}{\pi^{3/2}} \lambda + \frac{8}{9\pi^{3/2}} \lambda^3 + O(\lambda^5) \quad (19)$$

In turn, we use eqns. (18) and (19) to reduce eq. (15) to

$$\frac{1}{\pi} \int_{-1}^1 \frac{d\bar{\delta}/d\bar{s}}{\bar{x} - \bar{s}} d\bar{s} \approx \lambda \left(\frac{4}{\pi^{3/2}} - \frac{2}{\sqrt{\pi}} |\bar{x}| \right) + \lambda^3 \left(-\frac{8}{9\pi^{3/2}} + \frac{2}{3\sqrt{\pi}} |x|^3 \right) + O(\lambda^5) \quad (20)$$

We write the solution to the above equation as the perturbation expansion

$$\bar{\delta}(\bar{x}) \approx \lambda \delta_0(\bar{x}) + \lambda^3 \delta_1(\bar{x}) + O(\lambda^5) \quad (21)$$

where δ_0 and δ_1 satisfy

$$\frac{1}{\pi} \int_{-1}^1 \frac{d\delta_0/d\bar{s}}{\bar{x} - \bar{s}} d\bar{s} = \frac{4}{\pi^{3/2}} - \frac{2}{\sqrt{\pi}} |\bar{x}| \quad \frac{1}{\pi} \int_{-1}^1 \frac{d\delta_1/d\bar{s}}{\bar{x} - \bar{s}} d\bar{s} = -\frac{8}{9\pi^{3/2}} - \frac{2}{3\sqrt{\pi}} |\bar{x}|^3$$

The solutions to which

$$\delta_0(\bar{x}) = \frac{2}{\pi^{3/2}} \left(\sqrt{1-\bar{x}^2} - \bar{x}^2 \operatorname{atanh} \sqrt{1-\bar{x}^2} \right) \quad (22)$$

$$\delta_1(\bar{x}) = \frac{1}{3\pi^{3/2}} \left((\bar{x}^2 - 2)\sqrt{1-\bar{x}^2} + \bar{x}^4 \operatorname{atanh} \sqrt{1-\bar{x}^2} \right) \quad (23)$$

are found by the linear superposition of particular solutions to the general problem

$$g(x) = \frac{1}{\pi} \int_{-1}^1 \frac{h'(s)}{x-s} ds$$

that are provided in Table 3 and found following Appendix A. Using (21), the slip at the injection point in the marginally pressurized limit evaluates to

$$\delta(0) \approx \frac{\lambda \sqrt{\alpha t f} \Delta p}{\mu'} \left(\frac{2}{\pi^{3/2}} \lambda - \frac{2}{3\pi^{3/2}} \lambda^3 + O(\lambda^5) \right) \quad (24)$$

Table 3. Select solutions $h(x)$ to the problem $g(x) = \frac{1}{\pi} \int_{-1}^1 \frac{h'(s)}{x-s} ds$, with $h(\pm 1) = 0$.

$g(x)$	$h(x)$
1	$\sqrt{1-x^2}$
$\delta''_D(x)$	$\frac{1}{\pi} \frac{\sqrt{1-x^2}}{x^2}$
$\delta'_D(x)$	$-\frac{1}{\pi} \frac{\sqrt{1-x^2}}{x}$
$\delta_D(x)$	$\frac{1}{\pi} \operatorname{atanh} \sqrt{1-x^2}$
$\operatorname{sign}(x)/2$	$\frac{1}{\pi} x \operatorname{atanh} \sqrt{1-x^2}$
$ x - \frac{1}{\pi}$	$\frac{1}{\pi} x^2 \operatorname{atanh} \sqrt{1-x^2}$
$ x x$	$\frac{2}{3\pi} x^3 \operatorname{atanh} \sqrt{1-x^2} + \frac{2}{3\pi} x \sqrt{1-x^2}$
$ x ^3 - \frac{1}{3\pi}$	$\frac{1}{2\pi} x^4 \operatorname{atanh} \sqrt{1-x^2} + \frac{1}{2\pi} x^2 \sqrt{1-x^2}$

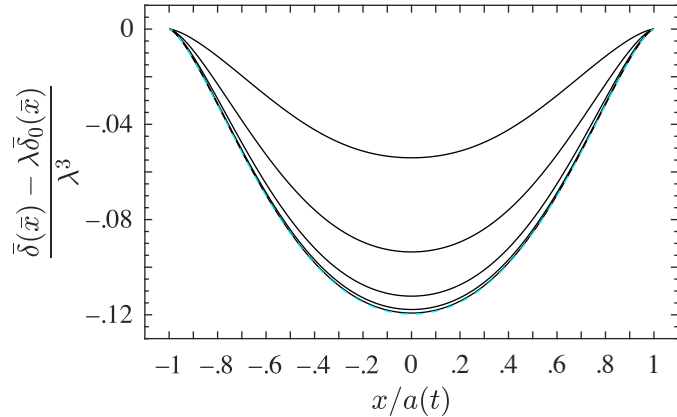


Fig. 5. Self-similar distribution of slip δ , less the first-order term, eq. (22), in the asymptotic expansion for slip eq. (21) in the marginally pressurized limit (small λ). From top to bottom, black curves correspond to the difference for $\lambda = 2, 1, \frac{1}{2}, \frac{1}{4}, \frac{1}{8}$. Cyan-dashed curve is the second-order term of the expansion, eq. (23)

5. Outer solution in the critically stressed limit

We now look for an asymptotic expansion of the solution in the critically stressed limit, in which the rupture front outpaces fluid pressure diffusion, $\lambda \gg 1$. As noted by GG12 for their problem, the solution consists of an outer solution on distances comparable to the rupture distance $a(t)$ and an inner solution on distances comparable to $\sqrt{\alpha}t$. To look for the outer solution we solve for the slip distribution satisfying eq. (15) after expanding the two terms on the left hand side in the large λ limit. We begin by considering the expansion of the following function as $\lambda \rightarrow \infty$

$$\frac{\operatorname{erfc}|u|}{\sqrt{1-(u/\lambda)^2}} \approx \operatorname{erfc}|u| + \frac{1}{2\lambda^2}u^2\operatorname{erfc}|u| + O(\lambda^{-4}) \quad (25)$$

This function appears in the integral (16) following the change of variable $u = \lambda\bar{x}$, such that

$$\left(1 - \frac{\tau}{\tau_p}\right) \frac{\sigma'}{\Delta p} = \frac{1}{\pi\lambda} \int_{-\lambda}^{\lambda} \frac{\operatorname{erfc}|u|}{\sqrt{1-(u/\lambda)^2}} du \approx \frac{2}{\pi^{3/2}} \frac{1}{\lambda} + \frac{1}{3\pi^{3/2}} \frac{1}{\lambda^3} + O(\lambda^{-5}) \quad (26)$$

In addition, we perform a multipole expansion of the distribution (Appendix B)

$$\operatorname{erfc}|\lambda\bar{x}| \approx p_0\delta_D(\bar{x}) - p_1\delta'_D(\bar{x}) + p_2\delta''_D(\bar{x}) + O(\lambda^{-5}) \quad (27)$$

where δ_D is the Dirac delta and its first and second derivatives, $\delta'_D(x)$ and $\delta''_D(x)$, with the properties

$$\int_{-\infty}^{\infty} \delta_D(x) dx = 1 \quad \int_{-\infty}^{\infty} x\delta'_D(x) dx = 1 \quad \int_{-\infty}^{\infty} \frac{x^2}{2}\delta''_D(x) dx = 1$$

and where the coefficients

$$p_0 = \int_{-1}^1 \operatorname{erfc}|\lambda\bar{x}| d\bar{x} = \frac{1}{\lambda} \int_{-\lambda}^{\lambda} \operatorname{erfc}|\hat{x}| d\hat{x} = \frac{2}{\sqrt{\pi}} \frac{1}{\lambda} + O(\exp(-\lambda^2)/\lambda) \quad (28)$$

$$p_1 = \int_{-1}^1 \bar{x}\operatorname{erfc}|\lambda\bar{x}| d\bar{x} = 0 \quad (29)$$

$$p_2 = \int_{-1}^1 \frac{\bar{x}^2}{2}\operatorname{erfc}|\lambda\bar{x}| d\bar{x} = \frac{1}{3\sqrt{\pi}} \frac{1}{\lambda^3} + O(\exp(-\lambda^2)/\lambda^3) \quad (30)$$

exhibit beyond-all-orders decay at large λ at the rate $\exp(-\lambda^2)$, following the leading-order term. With eqs. (26) and (27), the equation governing the slip distribution (15) becomes

$$\frac{1}{\pi} \int_{-1}^1 \frac{d\bar{\delta}/d\bar{s}}{\bar{x} - \bar{s}} d\bar{s} \approx \frac{1}{\lambda} \left(-\frac{2}{\pi^{3/2}} + \frac{2}{\sqrt{\pi}} \delta_D(\bar{x}) \right) + \frac{1}{\lambda^3} \left(-\frac{1}{3\pi^{3/2}} + \frac{1}{3\sqrt{\pi}} \delta''_D(\bar{x}) \right) + O(\lambda^{-5}) \quad (31)$$

As for the marginally pressurized case, we look for a solution in the form of a perturbation expansion

$$\bar{\delta}(\bar{x}) \approx \frac{1}{\lambda} \delta_0(\bar{x}) + \frac{1}{\lambda^3} \delta_1(\bar{x}) + O(\lambda^{-5}) \quad (32)$$

where δ_0 and δ_1 now satisfy

$$\frac{1}{\pi} \int_{-1}^1 \frac{d\delta_0/d\bar{s}}{\bar{x} - \bar{s}} d\bar{s} = -\frac{2}{\pi^{3/2}} + \frac{2}{\sqrt{\pi}} \delta_D(\bar{x}) \quad \frac{1}{\pi} \int_{-1}^1 \frac{d\delta_1/d\bar{s}}{\bar{x} - \bar{s}} d\bar{s} = -\frac{1}{3\pi^{3/2}} + \frac{1}{3\sqrt{\pi}} \delta''_D(\bar{x})$$

and the solutions

$$\delta_0(\bar{x}) = \frac{2}{\pi^{3/2}} \left(\operatorname{atanh} \sqrt{1 - \bar{x}^2} - \sqrt{1 - \bar{x}^2} \right) \quad (33)$$

$$\delta_1(\bar{x}) = \frac{1}{3\pi^{3/2}} \left(\frac{\sqrt{1 - \bar{x}^2}}{\bar{x}^2} - \sqrt{1 - \bar{x}^2} \right) \quad (34)$$

are again found by superposing solutions provided in Table 3.

From the above, the outer solution for slip near $\bar{x} = 0$ has the behavior

$$\delta(\bar{x}) \approx \frac{\lambda \sqrt{\alpha t} f \Delta p}{\mu'} \left[\frac{1}{\lambda} \frac{2}{\pi^{3/2}} \left(\log \frac{2}{|\bar{x}|} - 1 + \frac{\bar{x}^2}{4} + O(\bar{x}^4) \right) + \frac{1}{\lambda^3} \frac{1}{3\pi^{3/2}} \left(\frac{1}{\bar{x}^2} - \frac{3}{2} + O(\bar{x}^2) \right) + O(\lambda^{-5}) \right] \quad (35)$$

6. Inner solution in the critically stressed limit

To examine the behavior of slip on the diffusive lengthscale $\sqrt{\alpha t}$, we perform a change of variable to the scale distance $\hat{x} = \lambda \bar{x} = x/\sqrt{\alpha t}$, such that eq. (36) becomes

$$\lambda \frac{d\bar{\delta}}{d\hat{x}} = -\frac{\sqrt{1 - (\hat{x}/\lambda)^2}}{\pi} \int_{-\lambda}^{\lambda} \frac{\operatorname{erfc}|\hat{s}|}{\sqrt{1 - (\hat{s}/\lambda)^2}} \frac{1}{\hat{x} - \hat{s}} d\hat{s} \quad (36)$$

Rescaling slip as $\hat{\delta} = \lambda \bar{\delta} = \delta / (\sqrt{\alpha t} f \Delta p / \mu')$, we perform a series expansion of the square-root terms for large λ

$$\frac{d\hat{\delta}}{d\hat{x}} \approx -\frac{1}{\pi} \left(1 - \frac{1}{\lambda^2} \frac{\hat{x}^2}{2} + O(\lambda^{-4}) \right) \int_{-\lambda}^{\lambda} \left(\operatorname{erfc}|\hat{s}| + \frac{1}{\lambda^2} \frac{\hat{s}^2}{2} \operatorname{erfc}|\hat{s}| + O(\lambda^{-4}) \right) \frac{1}{\hat{x} - \hat{s}} d\hat{s} \quad (37)$$

and regroup terms of similar order

$$\frac{d\hat{\delta}}{d\hat{x}} \approx -\frac{1}{\pi} \int_{-\lambda}^{\lambda} \frac{\operatorname{erfc}|\hat{s}|}{\hat{x} - \hat{s}} d\hat{s} + \frac{1}{\lambda^2} \left(\frac{\hat{x}^2}{2} \frac{1}{\pi} \int_{-\lambda}^{\lambda} \frac{\operatorname{erfc}|\hat{s}|}{\hat{x} - \hat{s}} d\hat{s} - \frac{1}{\pi} \int_{-\lambda}^{\lambda} \frac{(\hat{s}^2/2)\operatorname{erfc}|\hat{s}|}{\hat{x} - \hat{s}} d\hat{s} \right) + O(\lambda^{-4}) \quad (38)$$

Given the beyond-all-orders decay, for modestly large values \hat{s} , of the term $\operatorname{erfc}|\hat{s}| \approx \exp(-\hat{s}^2)/(\sqrt{\pi}\hat{s})$ appearing in all of the integrands above, the limits of the integrals may pass to ∞ without consequence for the above expansion in powers of λ . Hence,

$$\frac{d\hat{\delta}}{d\hat{x}} \approx -\frac{1}{\pi} \int_{-\infty}^{\infty} \frac{\operatorname{erfc}|\hat{s}|}{\hat{x} - \hat{s}} d\hat{s} + \frac{1}{\lambda^2} \left(\frac{\hat{x}^2}{2} \frac{1}{\pi} \int_{-\infty}^{\infty} \frac{\operatorname{erfc}|\hat{s}|}{\hat{x} - \hat{s}} d\hat{s} - \frac{1}{\pi} \int_{-\infty}^{\infty} \frac{(\hat{s}^2/2)\operatorname{erfc}|\hat{s}|}{\hat{x} - \hat{s}} d\hat{s} \right) + O(\lambda^{-4}) \quad (39)$$

The above integrals are Hilbert transforms, defined as

$$\mathcal{H}[f(s)] = \frac{1}{\pi} \int_{-\infty}^{\infty} \frac{f(s)}{x-s} ds$$

which have the property

$$\begin{aligned} \mathcal{H}[s^2 f(s)] &= \mathcal{H}[(s^2 - x^2 + x^2)f(s)] \\ &= x^2 \mathcal{H}[f(s)] + \mathcal{H}[(s-x)(s+x)f(s)] \\ &= x^2 \mathcal{H}[f(s)] - \frac{1}{\pi} \int_{-\infty}^{\infty} s f(s) ds - \frac{x}{\pi} \int_{-\infty}^{\infty} f(s) ds \end{aligned}$$

that, when applied to the third integral in eq. (39)

$$\frac{1}{\pi} \int_{-\infty}^{\infty} \frac{(\hat{s}^2/2)\operatorname{erfc}|\hat{s}|}{\hat{x}-\hat{s}} d\hat{s} = \frac{\hat{x}^2}{2} \frac{1}{\pi} \int_{-\infty}^{\infty} \frac{\operatorname{erfc}|\hat{s}|}{\hat{x}-\hat{s}} d\hat{s} - \frac{\hat{x}}{\pi^{3/2}} \quad (40)$$

leads to the reduction of eq. (39) to

$$\frac{d\hat{\delta}}{d\hat{x}} \approx -\frac{1}{\pi} \int_{-\infty}^{\infty} \frac{\operatorname{erfc}|\hat{s}|}{\hat{x}-\hat{s}} d\hat{s} + \frac{1}{\lambda^2} \frac{\hat{x}}{\pi^{3/2}} + O(\lambda^{-4}) \quad (41)$$

Subsequently integrating from 0 to \hat{x} , we find the inner solution to within a yet-undetermined constant $\delta(0)$

$$\hat{\delta}(\hat{x}) \approx \hat{\delta}(0) - \underbrace{\int_0^{\hat{x}} \left[\frac{1}{\pi} \int_{-\infty}^{\infty} \frac{\operatorname{erfc}|s|}{x-s} ds \right] dx}_{\text{underlined term}} + \frac{1}{\lambda^2} \frac{\hat{x}^2}{2\pi^{3/2}} + O(\lambda^{-4}) \quad (42)$$

We define the underlined term as the function $f(\hat{x})$ whose first derivative is the Hilbert transform

$$f'(\hat{x}) = \frac{1}{\pi} \int_{-\infty}^{\infty} \frac{\operatorname{erfc}|s|}{\hat{x}-s} ds$$

Since the transform commutes with derivatives, $[\mathcal{H}(g)]' = \mathcal{H}(g')$, we find that f'' has the concise expression

$$f''(\hat{x}) = -\frac{2}{\pi^{3/2}} \int_{-\infty}^{\infty} \frac{\operatorname{sign}(s) \exp(-s^2)}{\hat{x}-s} ds$$

which may be further simplified

$$\begin{aligned} f''(\hat{x}) &= -\frac{2}{\pi^{3/2}} \exp(-\hat{x}^2) \int_0^{\infty} \frac{\exp(\hat{x}^2 - s^2)}{\hat{x}^2 - s^2} 2s ds \\ &= -\frac{2}{\pi^{3/2}} \exp(-\hat{x}^2) \int_{-\hat{x}^2}^{\infty} \frac{\exp(-u)}{u} du \\ &= -\frac{2}{\pi^{3/2}} \exp(-\hat{x}^2) \operatorname{Ei}(\tilde{x}^2) \end{aligned} \quad (43)$$

with the change of variable $u = s^2 - \hat{x}^2$ used in the intermediate step. In Figure 6 we plot $f(\hat{x})$ found by numerically integrating twice the expression for $f''(\hat{x})$, eq. (43).

For \hat{x} near 0,

$$f''(\hat{x}) = -\frac{2}{\pi^{3/2}} (\ln|\hat{x}| + \gamma) + O(\hat{x}^2)$$

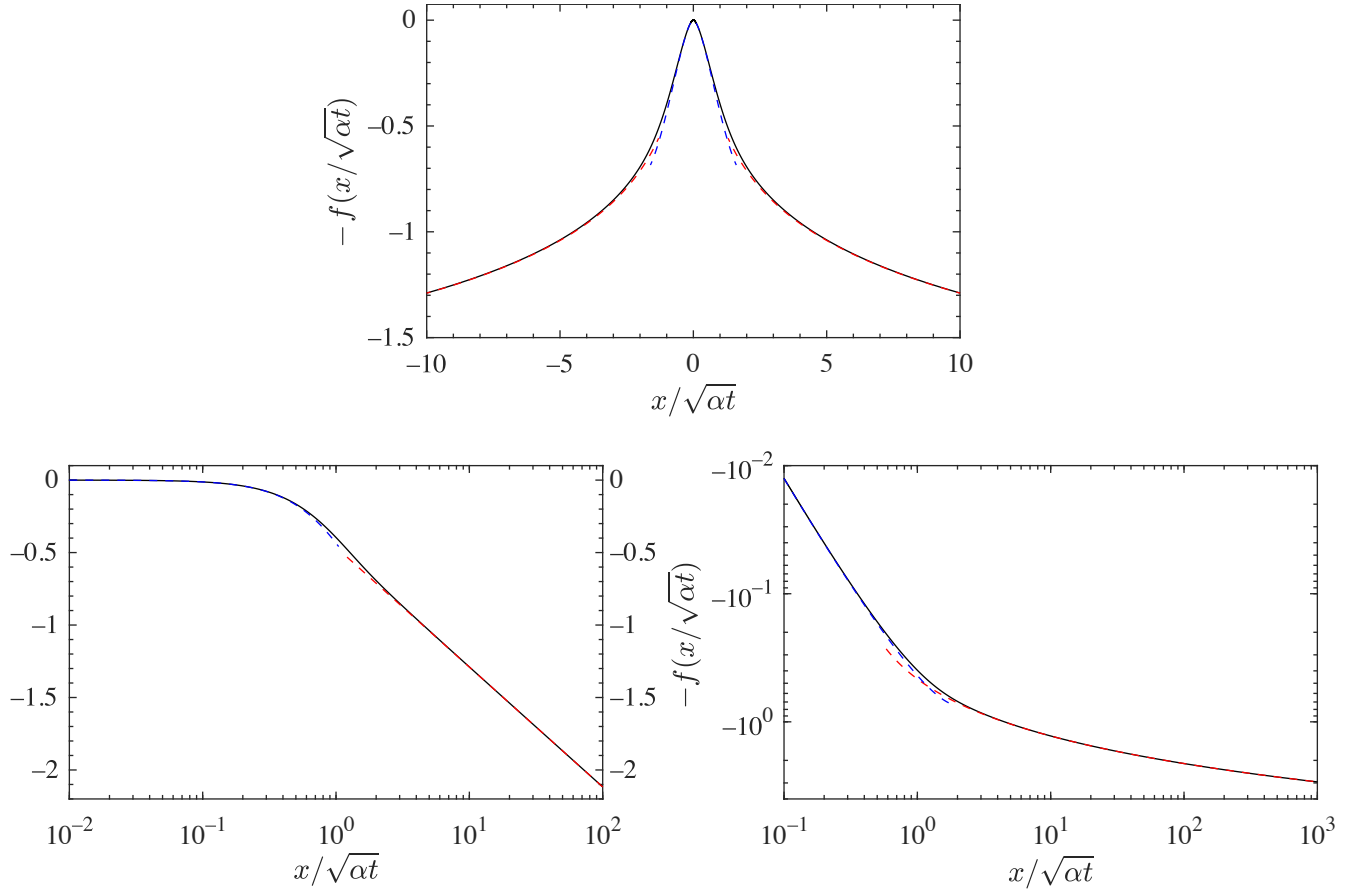


Fig. 6. Spatio-temporal component, $f(x/\sqrt{\alpha t})$, of “inner” solution for slip δ in the critically stressed limit, eq. (10). Shown on linear (**top**), log-linear (**left**), and logarithmic (**right**) axes. Red- and blue-dashed curves: outer and inner asymptotic behavior of f , eqs (11) and (13).

and upon integrating twice with $f(0) = f'(0) = 0$, the behavior of f in this region is

$$f(\hat{x}) = \frac{2}{\pi^{3/2}} \hat{x}^2 \left(\ln \frac{1}{|\hat{x}|} - \frac{\gamma}{2} + \frac{3}{2} \right) + O(\hat{x}^4 \ln |\hat{x}|)$$

For large \hat{x}

$$f''(\hat{x}) = -\frac{2}{\pi^{3/2}} \left(\frac{1}{\hat{x}^2} + \frac{1}{\hat{x}^4} \right) + O(\hat{x}^{-6})$$

Upon integrating twice with the condition that $f'(\infty) = 0$,

$$f(\hat{x}) = c + \frac{2}{\pi^{3/2}} \left(\ln |\hat{x}| - \frac{1}{6\hat{x}^2} \right) + O(\hat{x}^{-4}) \quad (44)$$

where c is a yet-undetermined constant of integration.

We determine the constant c following an approach used by *Garagash and Germanovich* [2012], in which the order of integration in eq. (42) is swapped leading to an alternative expression for $f(\hat{x})$

$$f(\hat{x}) = \int_0^{\hat{x}} \left[\frac{1}{\pi} \int_{-\infty}^{\infty} \frac{\operatorname{erfc}|s|}{x-s} ds \right] dx = \frac{1}{\pi} \int_{-\infty}^{\infty} \operatorname{erfc}|s| \ln \left| 1 - \frac{\hat{x}}{s} \right| ds \quad (45)$$

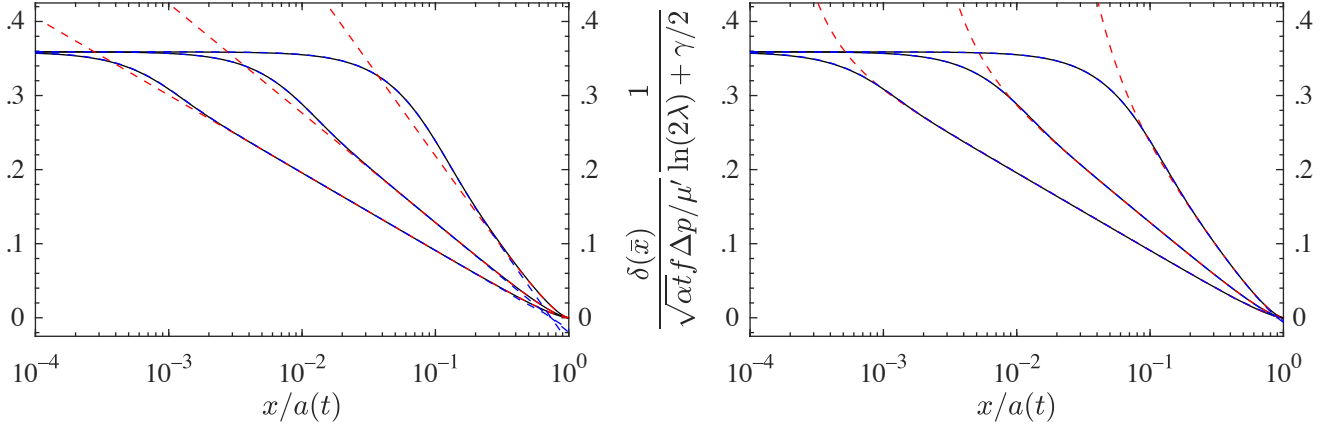


Fig. 7. Self-similar distribution of slip in the critically stressed limit (large λ). In this limit, the rupture extent $a(t)$ outpaces the diffusive distance $\sqrt{\alpha t}$. (**left and right**) Black curves from right to left correspond to full solutions self-similar slip profiles for $\lambda = 10, 100, 1000$. (**left**) Red-dashed and blue-dashed correspond to outer and inner solution expansion to first order. (**right**) Red-dashed and blue-dashed correspond to outer and inner solution expansion to second order. Outer solution is given by eqs. (32–34). Inner solution given by eqs. (42) and (48).

and the expansion $\ln|1 - \hat{x}/s| = \ln|\hat{x}| - \ln|s| + \ln|s/\hat{x} - 1|$ is used to decompose the latter integral for $f(\hat{x})$ into the sum

$$f(\hat{x}) = \frac{1}{\pi} \int_{-\infty}^{\infty} \operatorname{erfc}|s| ds \ln|\hat{x}| - \frac{1}{\pi} \int_{-\infty}^{\infty} \operatorname{erfc}|s| \ln|s| ds + \frac{1}{\pi} \int_{-\infty}^{\infty} \operatorname{erfc}|s| \ln\left|\frac{s}{\hat{x}} - 1\right| ds \quad (46)$$

$$= \frac{2}{\pi^{3/2}} \ln|\hat{x}| + \frac{2}{\pi^{3/2}} \left(1 + \frac{\gamma}{2}\right) + \frac{1}{\pi} \int_{-\infty}^{\infty} \operatorname{erfc}|s| \ln\left|\frac{s}{\hat{x}} - 1\right| ds \quad (47)$$

Comparing (44) and (47), we see that the asymptotic behavior of the last integral in (47), for large \hat{x} , is given by the terms in (44), excluding the constant and the logarithmic terms. We also retrieve the value of the constant c

$$c = \frac{2}{\pi^{3/2}} \left(1 + \frac{\gamma}{2}\right)$$

from which we conclude that the inner solution for slip has the asymptotic behavior at large \hat{x}

$$\delta(\hat{x}) \approx \delta(0) - \frac{\sqrt{\alpha t} f \Delta p}{\mu'} \left[\frac{2}{\pi^{3/2}} \left(1 + \frac{\gamma}{2} + \ln|\hat{x}| - \frac{1}{6|\hat{x}|^2} + O(\hat{x}^{-4})\right) - \frac{1}{\lambda^2} \frac{\hat{x}^2}{2\pi^{3/2}} + O(\lambda^{-4}) \right] \quad (48)$$

7. Matching inner and outer solutions

We match the outer and inner solutions by equating eqs. (35) and (48) and solving for $\delta(0)$, the slip at the center in the critically stressed limit

$$\delta(0) \approx \frac{\sqrt{\alpha t} f \Delta p}{\mu'} \frac{2}{\pi^{3/2}} \left[\frac{\gamma}{2} + \ln(2\lambda) - \frac{1}{4\lambda^2} + O(\lambda^{-4}) \right] \quad (49)$$

which completes the expression for the inner solution 42. In Fig. 7, we overlay the inner and outer solutions, to first and second order, above the full solutions for several large values of λ . The intermediate matching of the solutions is evident in the overlap of the dashed curves. As an aside, we can now show approximations to the slip at the center to first and second order in both the

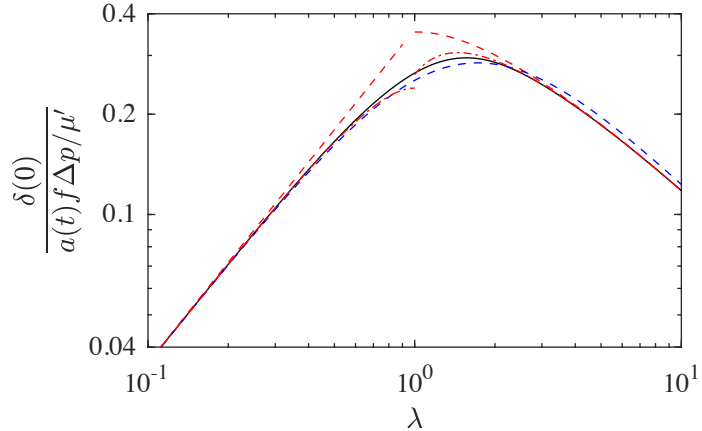


Fig. 8. Comparison of approximations to the full solution of peak fault slip (black curve) in the vicinity of $\lambda = 1$. First- and second- order approximations in the marginally pressurized and critically stressed limits, given respectively by eqs. (24) and (49), are shown as red-dashed and red-dot-dashed curves. Blue-dashed curve: approximation provided for all values of λ , eq. (14).

critically stressed and marginally pressurized limits in Fig. 8. For comparison, we also show the full solution and ad hoc approximation (14) constructed using the first-order asymptotics.

Using the inner and outer solutions, we construct a composite approximation [e.g., *Hinch*, 1991]

$$\delta_{comp}(\bar{x}) = \delta_{in}(\lambda\bar{x}) + \delta_{out}(\bar{x}) - \delta_{overlap}(\bar{x})$$

where δ_{in} and δ_{out} are the inner and outer solutions, eqs. (42) and (32), and

$$\delta_{overlap}(\bar{x}) = \frac{2}{\pi^{3/2}} \left(\log \frac{2}{\bar{x}} - 1 + \frac{\bar{x}^2}{4} \right) + \frac{1}{\lambda^2} \frac{1}{3\pi^{3/2}} \left(\frac{1}{\bar{x}^2} - \frac{3}{2} \right) + O(\lambda^{-4})$$

is their common intermediate form. In Fig. 9 we compare the full numerical solution against the inner, outer, and composite solutions for a modestly large value of $\lambda = 5$. The composite solution has an approximate error of $O(\lambda^{-(n+2)})$ where $n = 2$ or 4 is the order neglected in the asymptotic expansion.

8. Summary and conclusion

... has been studied in detail. Tracking the rupture of the fault corresponds to a free boundary problem for which both the size of the slipping domain and the distribution of slip must be solved. Both depend on a single dimensionless parameter whose limits correspond either to a fault whose initial, pre-injection shear stress is relatively close to the fault's pre-injection shear strength or to a fluid pressure increase that is marginally sufficient to induce sliding. Because the problem involves contact between elastic half-spaces, interactions between points on the fault are non-local, in that slip in one location induces changes in the shear stress over the entire fault plane, and the resulting governing equation is an integro-differential equation. In addition to the crack-tip boundary condition that slip vanish at the rupture front, the condition determining the free boundary is the absence of a stress singularity ahead of the rupture front, which corresponds to the boundary condition that the gradient of slip vanishes at the rupture front. Moreover, because the friction coefficient is held constant, there is an absence of an elasto-frictional lengthscale that may be otherwise present in problems for which friction depend explicitly on slip or its history. Correspondingly, the only lengthscale in the problem is the diffusive length \sqrt{at} with

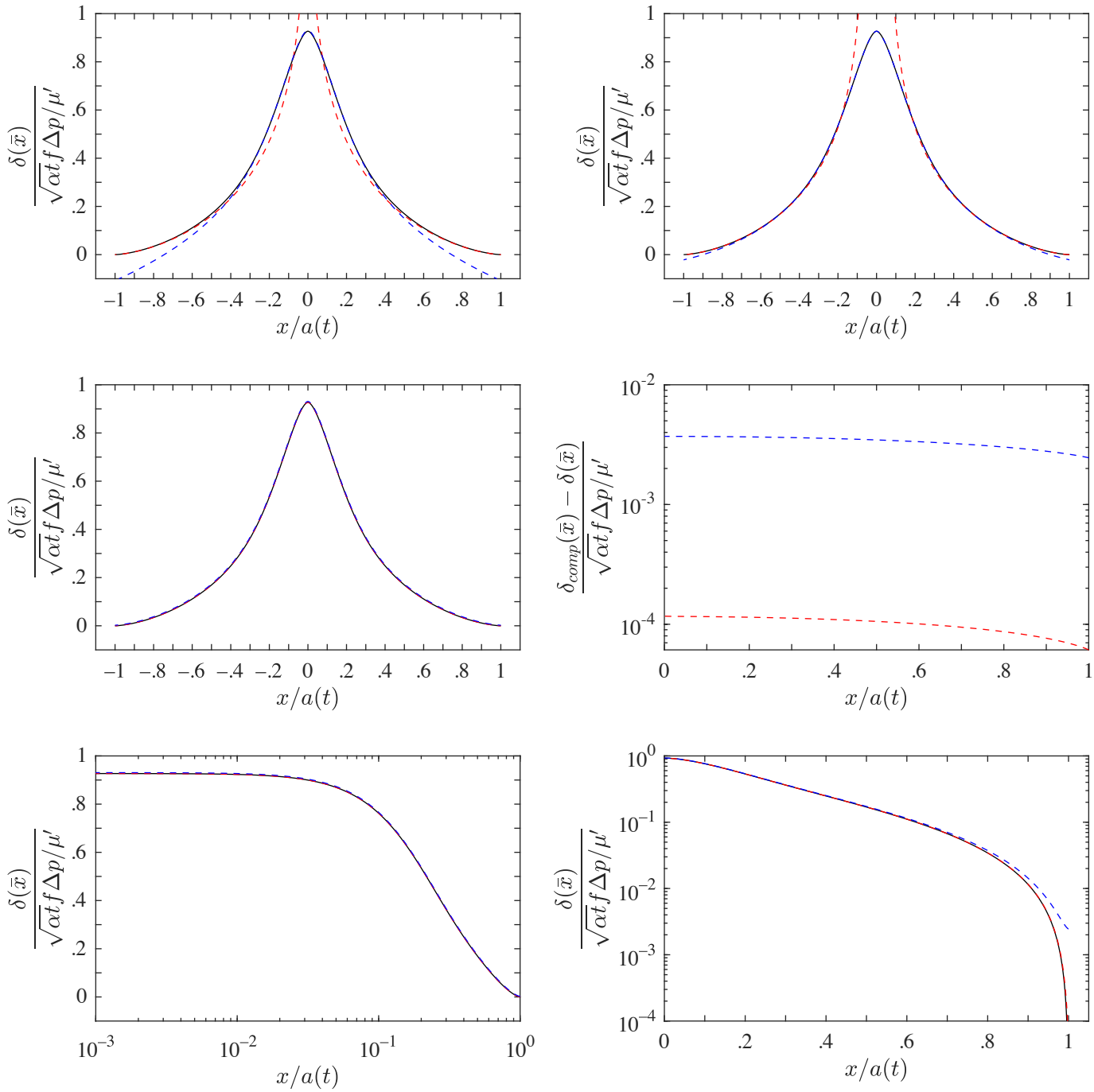


Fig. 9. Solution for self-similar slip profile in black for $\lambda = 5$. **(top)** superimposed blue- and red-dashed curves, respectively, showing inner and outer solutions to **(top-left)** leading and **(top-order)** next order. **(middle-left)** Superposition of leading and next-order composite solutions as blue- and red-dashed curves **(middle-right)**. The difference between the self-similar solution and the composite solutions at leading- and next-order, respectively blue and red-dashed curves. **(bottom)** Semi-logarithmic plots comparing the leading- and next-order composite solutions, in blue- and red-dashed, to the self-similar solution, in black.

the consequence that spatial dependence of slip scales directly with this lengthscale, implying the self-similar propagation of slip.

References

- Bhattacharya, P., and R. C. Viesca (2019) Fluid-induced aseismic fault slip outpaces pore-fluid migration, *Science*, 364, 464–468, doi:10.1126/science.aaw7354
- Erdogan F., Gupta G.D., Cook T.S. (1973) Numerical solution of singular integral equations. Ch. 7 from Sih, G.C. (ed.), *Methods of analysis and solutions of crack problems*. Mechanics of fracture, vol 1. Springer, Dordrecht, doi: 10.1007/978-94-017-2260-5_7
- Garagash, D. I., and L. N. Germanovich (2012), Nucleation and arrest of dynamic slip on a pressurized fault, *J. Geophys. Res.*, 117, B10310, doi:10.1029/2012JB009209
- Hinch, E. J. (1991), Perturbation Methods, *Cambridge University Press*, doi:10.1017/CBO9781139172189
- King, F. W. (2009) Hilbert Transforms, vols 1 & 2. *Cambridge University Press*, doi: 10.1017/CBO9780511721458 & 10.1017/CBO9780511735271
- Mushkhelishvili, N. I. (1958), Singular Integral Equations, *Springer*, Dordrecht, doi:10.1007/978-94-009-9994-7
- Viesca, R. C. and D. I. Garagash (2018), Numerical methods for coupled fracture problems, *J. Mech. Phys. Solids*, 113, 13–34, doi:10.1016/j.jmps.2018.01.008

Appendix A: Finite Hilbert transform solutions

The problem for slip posed as eq. (15) has the form of a finite Hilbert transform

$$g(x) = \frac{1}{\pi} \int_{-1}^1 \frac{h'(s)}{x-s} ds \quad (\text{A.1})$$

where, here, $g(x)$ corresponds to a prescribed loading and h of the distribution slip on the interface that is in quas-static equilibrium with the loading. The solution to eq. (A.1) has the known inversion [Mushkhelishvili, 1958; King, 2009]

$$h'(x) = \frac{C}{\sqrt{1-x^2}} - \frac{1}{\sqrt{1-x^2}} \frac{1}{\pi} \int_{-1}^1 \frac{\sqrt{1-s^2} g(s)}{x-s} ds \quad C = \frac{1}{\pi} \int_{-1}^1 h'(s) ds \quad (\text{A.2})$$

Since since slip vanishes at the rupture boundaries, the corresponding condition on h is $h(\pm 1) = 0$ and hence $C = 0$.

As an example solution, consider the distribution $g(x) = \delta_D(x)$, which is equivalent to a distribution of a point-force at the origin in the corresponding crack problem. The inversion for $h'(x)$ is

$$h'(x) = -\frac{1}{\sqrt{1-x^2}} \frac{1}{\pi} \int_{-1}^1 \frac{\sqrt{1-s^2} \delta_D(s)}{x-s} ds = -\frac{1}{\pi} \frac{1}{x \sqrt{1-x^2}} \quad (\text{A.3})$$

and integrating again with respect to x , with the condition $h(\pm 1) = 0$, we find that

$$h(x) = \frac{1}{\pi} \operatorname{arctanh} \sqrt{1-x^2} \quad (\text{A.4})$$

In Table 3, we present a number of similarly derived solutions from which we draw in the main text.

From eq. (A.2), we find that $h'(x)$ has the behavior in the limit $x \rightarrow \pm 1$

$$h'(x) = -\frac{1}{\sqrt{2(1 \pm x)}} \frac{1}{\pi} \int_{-1}^1 \sqrt{\frac{1 \mp s}{1 \mp s}} g(s) ds \quad (\text{A.5})$$

We may compare this behavior to the leading-order term in the Williams [1957] solution for slip near the tip of a crack located at $x = \pm a$

$$\delta(x) = \frac{K}{\mu'} \sqrt{\frac{2(a \mp x)}{\pi}} \quad \frac{d\delta}{dx} = \mp \frac{K}{\mu'} \sqrt{\frac{1}{2(a \mp x)}} \quad (\text{A.6})$$

where K is the conventionally defined mode-II or mode-III stress intensity factor and the corresponding leading order term in the distribution of stress ahead of the tip is $\tau_{tip}(x) = K/\sqrt{2\pi(x \pm a)}$. We may define a quantity k corresponding to the stress intensity factor K by $k = K/(\mu' \sqrt{a})$, and in comparing the latter expression in (A.6) with eq. (A.5), we can derive an analogous expression for an intensity factor k_{\pm} at $x = \pm 1$

$$k_{\pm} = \frac{1}{\sqrt{\pi}} \int_{-1}^1 \sqrt{\frac{1 \pm s}{1 \mp s}} g(s) ds$$

Requiring that this intensity factor vanish at both tips, hence implies that two conditions be satisfied by the distribution $g(s)$

$$\int_{-1}^1 \sqrt{\frac{1 \pm s}{1 \mp s}} g(s) ds = 0$$

which can be recast as the sum and the difference of these two conditions, leading respectively to

$$\int_{-1}^1 \frac{g(s)}{\sqrt{1-s^2}} ds = 0 \quad \int_{-1}^1 \frac{sg(s)}{\sqrt{1-s^2}} ds = 0 \quad (\text{A.7})$$

In the problem for the slip distribution, eq. (15), we identify

$$g(s) = \operatorname{erfc} |\lambda s| - \left(1 - \frac{\tau}{\tau_p}\right) \frac{\sigma'}{\Delta p} \quad (\text{A.8})$$

The first condition of (A.7) to be satisfied by (A.8) corresponds to eq. (16) in main text, which provides the direct relation between λ and the problem parameter $(1 - \tau/\tau_p)\sigma'/\Delta p$. The second condition of (A.7) is trivially satisfied by (A.8).

The non-singular stress conditions (A.7), if present, can be taken into account in the inversion for $h'(x)$, eq. (A.2), which may be rewritten as

$$\begin{aligned} h'(x) &= -\frac{1}{\sqrt{1-x^2}} \frac{1}{\pi} \int_{-1}^1 \frac{\sqrt{1-s^2} g(s)}{x-s} ds + \frac{1}{\sqrt{1-x^2}} \frac{1}{\pi} \int_{-1}^1 \frac{(x+s)g(s)}{\sqrt{1-s^2}} ds \\ &= -\frac{\sqrt{1-x^2}}{\pi} \int_{-1}^1 \frac{1}{\sqrt{1-s^2}} \frac{g(s)}{x-s} ds \end{aligned} \quad (\text{A.9})$$

Upon substituting eq. (A.8) in eq. (A.9), the contribution of the constant parameter $(1 - \tau/\tau_p)\sigma'/\Delta p$ vanishes, and we retrieve eq. (36) in the main text.

As another example, we again consider the distribution $g(x) = \delta_D(x)$, for which the inversion for $h'(x)$ with the non-singular condition on $h'(x)$ is

$$\begin{aligned} h'(x) &= \frac{-\sqrt{1-x^2}}{\pi} \int_{-1}^1 \frac{1}{\sqrt{1-s^2}} \frac{\delta_D(s)}{x-s} ds = -\frac{1}{\pi} \frac{\sqrt{1-x^2}}{x} = -\frac{1}{\pi} \left(\frac{1}{x\sqrt{1-x^2}} - \frac{x}{\sqrt{1-x^2}} \right) \\ h(x) &= \frac{1}{\pi} \left(\operatorname{arctanh} \sqrt{1-x^2} - \sqrt{1-x^2} \right) \end{aligned} \quad (\text{A.10})$$

to which we may compare, eq. (A.4), the inversion for the same distribution $g(x)$ without the non-singular condition.

In writing an asymptotic expansion for slip in powers λ in the marginally pressurized and critically stressed limits, we derived spatial distributions for slip at each order using results presented in Table 3. Note that while the compilation of results in Table 3 did not incorporate the non-singular crack conditions (A.7) in the inversion for $h'(x)$ from $g(x)$, the non-singular conditions are implicitly incorporated in the expansion for the stress parameter $(1 - \tau/\tau_p)\sigma'/\Delta p$ in terms of λ . The result is fully equivalent to the solution that would have been found had the conditions (A.7) been incorporated directly into the inversion. We recognize this, for instance, in noting that the first term in the expansion for slip in the critically-stressed limit, eq. (33), is given, to within the factor $p_0 = 2/\sqrt{\pi}$ by eq. (A.10).

Appendix B: Multipole expansion

Here we derive the multipole expansion of eqs. (27–30). This expansion was used to derive the outer solution in the critically stressed limit, for which the rupture extent $a(t) \gg \sqrt{\alpha t}$, such that the fluid pressure source appears localized about the origin. We begin by noting that the the solution to the problem for $h(x)$

$$g(x) = \frac{1}{\pi} \int_{-1}^1 \frac{h'(s)}{x-s} ds \quad (\text{B.1})$$

with the boundary conditions $h(-1) = h(1) = 0$, may be also written in terms of the Green's function $G(x, x')$ satisfying

$$\delta_D(x - x') = \frac{1}{\pi} \int_{-1}^1 \frac{G(s, x')}{x - s} ds$$

Using the inversion eq. (A.2), the Green's function is

$$\begin{aligned} G(x, x') &= -\frac{1}{\sqrt{1-x^2}} \frac{1}{\pi} \int_{-1}^1 \frac{\sqrt{1-s^2} \delta_D(s - x')}{x - s} ds \\ &= -\frac{1}{\pi} \sqrt{\frac{1-x'^2}{1-x^2}} \frac{1}{x - x'} \end{aligned} \quad (\text{B.2})$$

and the solution to eq. (B.1) can be written as

$$h'(x) = \int_{-1}^1 G(x, x') g(x') dx' \quad (\text{B.3})$$

We derive a multipole expansion for eq. (B.1) by considering that a Taylor series expansion of the Green's function in eq. (B.3) about the origin $x' = 0$

$$h'(x) = \int_{-1}^1 \left[G(x, 0) + x' \left. \frac{\partial G}{\partial x'} \right|_{x'=0} + \frac{x'^2}{2} \left. \frac{\partial^2 G}{\partial x'^2} \right|_{x'=0} + \dots + \frac{x'^n}{n!} \left. \frac{\partial^n G}{\partial x'^n} \right|_{x'=0} \right] g(x') dx'$$

reduces to

$$h'(x) = p_0 G(x, 0) + p_1 \left. \frac{\partial G}{\partial x'} \right|_{x'=0} + p_2 \left. \frac{\partial^2 G}{\partial x'^2} \right|_{x'=0} + \dots + p_n \left. \frac{\partial^n G}{\partial x'^n} \right|_{x'=0} \quad (\text{B.4})$$

where the coefficients of this series are

$$p_0 = \int_{-1}^1 g(x') dx', \quad p_1 = \int_{-1}^1 x' g(x') dx', \quad p_2 = \int_{-1}^1 \frac{x'^2}{2} g(x') dx', \quad \dots, \quad p_n = \int_{-1}^1 \frac{x'^n}{n!} g(x') dx'$$

The expansion of $g(x)$ implied by eq. (B.4) is found by first noting that, from eq. (B.2),

$$\frac{\partial^n G}{\partial x'^n} = -\frac{1}{\sqrt{1-x^2}} \frac{1}{\pi} \int_{-1}^1 \frac{\sqrt{1-s^2} [(-1)^n \delta_D^{(n)}(s - x')]}{x - s} ds \quad (\text{B.5})$$

where $\delta^{(n)}$ is the n -th derivative of δ_D with respect to its argument. When evaluating eq. (B.5) at $x' = 0$ and comparing with eq. (A.2), we see that eq. (B.5) is the inverted solution for $h'(x)$ when $g(x) = (-1)^n \delta_D^{(n)}(x)$, hence substituting eq. (B.4) into eq. (B.1) yields

$$g(x) = p_0 \delta_D(x) - p_1 \delta'_D(x) + p_2 \delta''_D(x) - \dots + (-1)^n p_n \delta_D^{(n)}(x)$$

where the leading two terms are the source monopole and dipole approximations, respectively. For $n = 0, 1, 2$, the first few functions of x in eq. (B.4) are

$$G(x, 0) = -\frac{1}{\pi} \frac{1}{x \sqrt{1-x^2}}, \quad \left. \frac{\partial G}{\partial x'} \right|_{x=0} = -\frac{1}{\pi} \frac{1}{x^2 \sqrt{1-x^2}}, \quad \left. \frac{\partial^2 G}{\partial x'^2} \right|_{x=0} = \frac{x^2 - 2}{x^3 \sqrt{1-x^2}}$$

Multiplying these functions by $(-1)^n$ and integrating with respect to x , we find the expressions in Table 3 for $h(x)$ when $g(x) = \delta_D(x)$ or one of its first two derivatives.